

PERFORMANCE EVALUATION OF NONLINEAR VISCOELASTIC MATERIALS USING FINITE ELEMENT METHOD

Laith Abed Sabri^{1,2,3*}, Adnan Naji Jameel Al-Tamimi³, Fathi A. Alshamma⁴,
M. N. Mohammed⁵, Kareem N Salloomi⁶, Oday I. Abdullah^{7,5,8}

¹Training and Workshop Center, University of Technology-Iraq, Baghdad 10001, IRAQ

²Department of Mechatronics, Al-Khwarizmi College of Engineering, University of Baghdad, Baghdad, IRAQ

³College of Technical Engineering, Al-Farahidi University, IRAQ

⁴Mechanical Engineering Department, College of Engineering, University of Baghdad, IRAQ

⁵Mechanical Engineering Department, College of Engineering, Gulf University, Sanad 26489, BAHRAIN

⁶Automated Manufacturing Engineering Department, Al-Khwarizmi College of Engineering, University of Baghdad, Baghdad, IRAQ

⁷Energy Engineering Department, College of Engineering, University of Baghdad, Baghdad 10071, IRAQ

⁸Department of Mechanics, Al-Farabi Kazakh National University, Almaty 050040, KAZAKHSTAN
E-mail: laith@kecbu.uobaghdad.edu.iq

This research paper applies the finite element method as a methodology to evaluate the structural performance of nonlinear viscoelastic solids. A finite element algorithm was built and developed to simulate the mathematical nonlinear viscoelastic material behavior based on incremental constitutive equations. The derived Equation of the incremental constitutive included the complete strain and stress histories. The Schapery's nonlinear viscoelastic material model was integrated within the displacement-based finite element environment to perform the analysis. A modified Newton-Raphson technique was used to solve the nonlinear part in the resultant equations. In this work, the deviatoric and volumetric strain–stress relations were decoupled, and the hereditary strains were updated at the end of each time increment. It is worth mentioning that the developed algorithm can be effectively employed for all the permissible values of Poisson's ratio by using a selective integration procedure. The algorithm was tested for a number of applications, and the results were compared with some previously published experimental results. A small percentage error of (1%) was observed comparing the published experimental results. The developed algorithm can be considered a promising numerical tool that overcomes convergence issues, enhancing equilibrium with high-accuracy results.

Key words: finite element method; viscoelastic; nonlinear analysis; uniaxial and multiaxial stresses formulation.

1. Introduction

One of the fundamental factors in choosing any successful design for a structure is assigning suitable material properties [1, 2]. The viscoelastic material behavior could appear in different materials and a wide

* To whom correspondence should be addressed

range of applications [3]. Moreover, structural materials like polymers, turbine blades, solid propellant rocket fuels, soil mechanics, and even some biological parts like bones and soft tissues may behave as viscoelastic material [4]. Most of the previously published studies within the viscoelastic materials field showed that polymeric materials' behavior mainly depends on time and other effective factors such as applied load, working temperature, and moisture [5]. Structure performance analysis of nonlinear viscoelastic solids is used in several fields, starting from material design and biomechanics to manufacturing. It helps to optimize the material for durability while understanding the viscoelastic behavior of biological tissues as well as predicting the long-term performance of engineered structures. Thus contributing to increased reliability and performance across various applications such as aerospace, automotive, and medical devices.

In fact, there are two main ways to describe viscoelastic material behavior, linear and nonlinear [6,7]. The relation between stress and strain is linear for linear viscoelastic material behavior. Many researchers adopted the finite element method to study the linear viscoelastic behavior of their materials [8]. In viscoelastic material, the constitutive equations may be represented in either differential form [1] or integral form [9]. Most of the finite element developers used the integral form [10]. Zobeiry [11] extended the one-dimensional linear formulation into the three-dimensional behavior of both isotropic and transversely isotropic viscoelastic materials. Zobeiry implemented the constitutive finite element formulation by using Abaqus as a user material model, and the study was verified through the simulation of some numerical cases. Tressou *et al.* [3] applied the incremental variational approach (EIV model) to describe the linear viscoelastic behavior of different types of composite material like long fiber, particle-reinforced, and strand-based composites.

On the other hand, Schapery's model [12] is one of the common models to describe nonlinear viscoelastic material. Henriksen [4] was one of the first authors who applied the Schapery representation in FEM to achieve the multiaxial stress analysis. In order to account for more accurate viscoelastic material behavior during loading conditions, nonlinear effects due to temperature and physical aging were considered in the work of Lai and Bakker [6]. The authors modified Henriksen recursive algorithm by using reduced time functions. Also, the deviatoric and volumetric parts were decoupled by considering isotropic material. The study used the constitutive formulation to model experimental tests carried out on PMMA polymer for validation purposes. Rami and Muliana [5] presented a numerical integration method for the nonlinear viscoelastic behavior of isotropic materials and structures. They started with Lai and Bakker [6] experimental results as a verification case. In this work, the recursive integration method was applied for the constitutive formulation but with a new iterative style and predictor-corrector type steps. The constitutive equations were extracted in a step-by-step form, assuming a constant incremental strain rate. This recursive formulation allowed updating the hereditary strains at the end of each time increment. Rami and Muliana [7, 8, 13, 14] Modified their work to simulate the micromechanical approach for the nonlinear viscoelastic behavior of pultruded composites. Huang [15] represented the asphalt pavement behavior using nonlinear viscoelastic and viscoplastic Schapery's model. An Abaqus code, UMAT, was used to represent the asphalt's nonlinear viscoelastic and viscoplastic behavior. The three-dimensional model was represented using three three-layer structures, and different thermal loading was applied.

Muliana and Rami [9] developed a finite element code to solve the nonlinear thermo-viscoelastic of multi-layered and thick-section composite plates. They demonstrated two alternating fiber-reinforced polymeric layers: unidirectional fiber (roving) and continuous filament mat (CFM). Periodic boundary conditions are formulated for the roving and CFM to simplify 3D micromechanical models.

Rahmani *et al.* [16] used the Schapery model to describe the stress/strain behavior of asphalt concrete. The study proved that the confinement pressure highly affected the nonlinear viscoelastic response of asphalt concrete materials. In order to find the nonlinear parameters for Schapery models, the study used cyclic creep-recovery tests at 55°C and at different confinement levels.

In the last decade, the behavior of some of the biological parts, like bones and soft tissues, were described using viscoelastic material. Peña *et al.* [17] developed a constitutive law to describe the mechanical behavior of the vascular tissue. The proposed models within this study took into consideration all the material features of the vascular tissues by applying the concept of composite material. The developed models also considered strain-dependent reduced relaxation and time functions and different viscoelastic parameters for the matrix and the fibers. Huang *et al.* [15] used the Abaqus user material subroutine UMAT to describe the

response of the asphalt mixtures under different temperatures and rates of loading. The study represents the material model as a nonlinear viscoelastic-viscoplastic. The study also represents the asphalt mixtures as a three-layer pavement structure to simulate the asphalt responses under repeated loading at different temperatures. Feng *et al.* [18] studied the mechanical behavior of the elastomer; they assumed the constitutive Equation for the model is the nonlinear viscoelastic model. The Finite element simulation is implemented using Abaqus software, and they developed the user-defined material (UMAT) subroutine. The Finite Element software's validity and modeling ability are done with some numerical examples under different loading conditions. Takaoka [19] investigated the mechanical behavior of thermoplastic materials. In their study, they assumed polybutylene terephthalate (PBT) behavior is nonlinear viscoelastic-viscoplastic time-dependent materials. Therefore, they used Schapery nonlinear viscoelasticity and Perzyna viscoplasticity. The nonlinearity in the material behavior was solved using the finite element software Abaqus by implementing the Umat subroutine.

Many researchers [20-25] applied the finite element analysis to achieve different analyses about the viscoelastic behavior in different topics such as the dynamic response of orthotropic viscoelastic composite laminates plate, impact response of viscoelastic-frictionless bodies, Dynamic response of viscoelastic functionally graded porous thick beam and the analysis of viscoelastic bonding layer on the behavior of piezoelectric actuator.

In this research paper, a numerical model of nonlinear viscoelastic based on the Schapery type was developed. The strain rate was assumed to be constant for each increment of the developed program. This assumption is acceptable and didn't affect the accuracy of the results. It is also necessary to explain that the current model used a two-step numerical algorithm and achieved recursive integration. The last step involved minimizing the strain residual by updating the stresses. The obtained tangent stiffness matrix based on the developed algorithm was simple and consistent. The developed algorithm has the feature of overcoming the convergence issue and enhancing the equilibrium. A modified Newton-Raphson method was used to find the solution at each time step. In order to verify the finite element developed code, experimental data from Lai and Bakker[6] was used as a verification example.

2. Nonlinear viscoelastic modeling method

2.1. Uniaxial formulation of nonlinear viscoelastic

The uniaxial integral form of the Schapery equation for the current strain can be written as follows [2]:

$$\varepsilon(t) = g_o^{\sigma^t} D_o \sigma^t + g_l^{\sigma^t} \int_o^t \Delta D[\psi(t) - \psi(\tau)] \frac{d(g_2^{\sigma^t} \sigma^t)}{d\tau} d\tau. \quad (2.1)$$

The form of reduced time (effective time) is [2],

$$\psi(t) = \int_o^t \frac{ds}{a_\sigma a_T}. \quad (2.2)$$

The superscript (upper right) denoted the explicit variable. The properties of the nonlinear material (g_o , g_l , g_2 and a_σ) can be referred to as the nonlinear stress functions, the reason for this assumption is that they depend just on the stress variables (e.g. octahedral shear stress). In the case where the stress values are relatively small, the functions are equal to (+I) [Boltzmann integral in linear viscoelasticity].

a_σ and a_T are the time-scaling factor and temperature dependent. It can be used a_σ in thermorheologically simple materials to define the time scale shift factor. When included the temperature effect in Eq.(2.1), the viscoelastic behavior of a thermorheologically complex material can be yielded. Also, it can be included other

effects in Eq.(2.2), such as physical aging and moisture effects, by adding their functions (time-scaling). In the proposed analysis, only the nonlinearity according to stress is considered. g_o represents the nonlinear instantaneous elastic compliance, which indicates the change in the structure's stiffness. The nonlinearity effect in the transient compliance can be measured based on the transient creep parameter g_l . It can be calculated the effect of creep response which affected by the load rate based on the parameter g_2 . It was used the general polynomial functions of the shear stress (effective octahedral) to represent all nonlinear parameters the functions of the nonlinear parameters can be written as [6],

$$g_o = I + \sum_{i=1}^{ng_0} \alpha_i \left\langle \frac{\bar{\sigma}}{\sigma_o} - I \right\rangle^i, \quad g_l = I + \sum_{i=1}^{ng_l} \beta_i \left\langle \frac{\bar{\sigma}}{\sigma_o} - I \right\rangle^i, \quad g_2 = I + \sum_{i=1}^{ng_2} \gamma_i \left\langle \frac{\bar{\sigma}}{\sigma_o} - I \right\rangle^i, \quad (2.3)$$

$$a_\sigma = I + \sum_{i=1}^{na_\sigma} \delta_i \left\langle \frac{\bar{\sigma}}{\sigma_o} - I \right\rangle^i, \quad \psi(t) = \frac{t}{a_\sigma},$$

where

$$\langle x \rangle = \begin{cases} x, & x > 0, \\ 0, & x \leq 0. \end{cases} \quad (2.4)$$

It can be calibrated the coefficients ($\alpha_i, \beta_i, \gamma_i, \delta_i$) from recovery and creep tests. The range of the end for the linear viscoelastic can be calculated based on the effective stress limit (σ_o) [7]. ΔD and D_0 are the uniaxial transient compliance and the instantaneous uniaxial elastic compliance. The form of the uniaxial transient compliance using a Prony series is [6],

$$\Delta D \psi(t) = \sum_{n=1}^N D_n [1 - \exp(-\lambda_n \psi)] \quad (2.5)$$

where N, D_n , and λ_n are the numbers of terms, and the n^{th} coefficient is included in the Prony series and the n^{th} reciprocal of retardation time.

2.2. Numerical integration

This section presents the full details of the numerical integration formulation used in this analysis. After the numerical driving, the nonlinear viscoelastic constitutive model (isotropic materials) uses the single integral constitutive model (Schapery [2]).

It can be stored the data (incremental and integration) of the current stress at the earlier and current time step in addition to the strain increments, where the convolution integral splits into recursive elements. The iterative scheme was used to fulfill the assumptions for nonlinear viscoelastic integral when presented in expressions of stress-based variables. The iterative scheme was used to reduce the existing error in the recurrence integration. Applying the general polynomial form to represent the nonlinear parameters was suggested. It was achieved by the iterative correction algorithm simultaneously at the constitutive stage. In order to determine the current stress and strain of the polymer, it should have enough information about the history of stress and strain overloading. Owing to the time-dependent behavior and the existence of nonlinearity in the stress-strain relation, the relation of the incremental stress-strain for nonlinear viscoelastic materials is required. Therefore, the formulation of incremental for the constitutive equation should be

developed by applying a suitable integration procedure. The discontinuity at $t=0$ may be eliminated from Eq.(2.1) to obtain the following expression [6]:

$$\varepsilon(t) = g_o^{\sigma^t} D_o \sigma^t + g_l^{\sigma^t} g_2^{\sigma^t} \Delta D \Psi(t) \sigma^t + g_l^{\sigma^t} \int_{o^+}^t \Delta D[\Psi(t) - \Psi(\tau)] \frac{d(g_l^{\sigma^t} \sigma^t)}{d\tau} d\tau. \quad (2.6)$$

Integration by parts theorem can be applied to the second term to simplify the above equation into [6]:

$$\varepsilon(t) = g_o^{\sigma^t} D_o \sigma^t - g_l^{\sigma^t} \int_{o^+}^t \frac{d\{\Delta D[\Psi(t) - \Psi(\tau)]\}}{d\tau} g_2^{\sigma^t} \sigma^t d\tau. \quad (2.7)$$

In order to calculate the viscoelastic strain at the end of a time step, numerical integration was used. For the second term of Eq.(2.7),

$$\varepsilon(t_k) = g_o(t_k) D_o \sigma(t_k) - g_l(t_k) \int_{o^+}^{t_k} \frac{d\{\Delta D[\Psi(t_k) - \Psi(\tau)]\}}{d\tau} g_2(t_k) \sigma(t_k) d\tau. \quad (2.8)$$

By spite Eq.(2.8) into two parts, it can yield the form of recursive integration. The initial segment incorporates the integration [limits $(0, t_{k-1})$], i.e., until the earlier time step. In the second part, the limits were (t_{k-1}, t_k) . t represents the current time. Then [6],

$$\begin{aligned} & \int_{o^+}^t \frac{d\{\Delta D[\Psi(t_k) - \Psi(\tau)]\}}{d\tau} g_2(t_k) \sigma(t_k) d\tau = \\ & = \int_{o^+}^{t_{k-1}} \frac{d\{\Delta D[\Psi(t_{k-1}) - \Psi(\tau)]\}}{d\tau} g_2(t_k) \sigma(t_k) d\tau + \\ & + \int_{t_{k-1}}^{t_k} \frac{d\{\Delta D[\Psi(t_k) - \Psi(\tau)]\}}{d\tau} g_2(t_k) \sigma(t_k) d\tau. \end{aligned} \quad (2.9)$$

The first part of the Eq.(2.9) can be evaluated as follows:

$$\begin{aligned} & \int_{o^+}^{t_{k-1}} \frac{d\{\Delta D[\Psi(t_k) - \Psi(\tau)]\}}{d\tau} g_2(t_k) \sigma(t_k) d\tau = \\ & = \sum_{j=1}^{k-2} \int_{t_j}^{t_{j+1}} \frac{d\{\Delta D[\Psi(t_{j+1}) - \Psi(t_j)]\}}{d\tau} g_2(t_j) \sigma(t_j) d\tau. \end{aligned} \quad (2.10)$$

It can be achieved integration by part of the second term of Eq.(2.10) when we suppose that the various changes linearly over the current time step. Also, the change of the expression (g_2, σ) is linear over the increment of the current time step. It can be reduced in the second part of the integration when assuming that the shift parameter is indirectly a function of time as follows [7],

$$\begin{aligned}
&= \frac{I}{2} \sum_{j=1}^{k-1} \{g_2(t_{j+1})\sigma(t_{j+1}) + g_2(t_j)\sigma(t_j)\} \\
&\sum_{j=1}^{k-2} \int_{t_j}^{t_{j+1}} \frac{d\{\Delta D[\Psi(t_{j+1}) - \Psi(t_j)]\}}{d\tau} g_2(t_j)\sigma(t_j) d\tau.
\end{aligned} \tag{2.11}$$

Then it's equal to,

$$= \frac{I}{2} \sum_{j=1}^{k-2} \{g_2(t_{j+1})\sigma(t_{j+1}) + g_2(t_j)\sigma(t_j)\} \{\Delta D(\Delta\Psi(t_k - t_{j+1})) - \Delta D(\Delta\Psi(t_k - t_j))\}, \tag{2.12}$$

and for the second on the right side of Eq.(2.9),

$$\begin{aligned}
&\int_{t_{k-1}}^{t_k} \frac{d(\Delta D[\Psi(t_k) - \Psi(\tau)])}{d\tau} g_2(t_k)\sigma(t_k) d\tau = \\
&= \frac{I}{2} \{g_2(t_k)\sigma(t_k) + g_2(t_{k-1})\sigma(t_{k-1})\} \{\Delta D(\Delta\Psi(0)) - \Delta D(\Delta\Psi(t_k - t_{k-1}))\},
\end{aligned} \tag{2.13}$$

where

$$\Delta D[\Delta\Psi(0)] = 0. \tag{2.14}$$

By rearranging and substituting Eqs (2.14) into Eq.(2.8), it can be yielded the current strain (total strain):

$$\begin{aligned}
\varepsilon(t_k) &= g_o(t_k) D_o \sigma(t_k) + \frac{I}{2} g_l(t_k) \Delta D(\Psi(t_k - t_{k-1})) \\
&\{g_2(t_k)\sigma(t_k) + g_2(t_{k-1})\sigma(t_{k-1})\} - \frac{I}{2} g_l \sum_{j=1}^{k-2} \Delta D(\Psi(t_k - t_{j+1})) + \\
&- \Delta D(\Psi(t_k - t_j)) \{g_2(t_{j+1})\sigma(t_{j+1}) + g_2(t_j)\sigma(t_j)\}.
\end{aligned} \tag{2.15}$$

The stress-strain relation could be written in the form [7],

$$\varepsilon(t) = g_o(t_k) D_o \sigma(t_k) + \frac{I}{2} g_l(t_k) \Delta D(\Psi(t_k - t_{k-1})) \sigma(t_k) + H(t_k), \tag{2.16}$$

where $H(t)$ is the hereditary integration form, as shown below [7],

$$\begin{aligned}
H(t_k) &= \frac{I}{2} g_l(t_k) \Delta D(\Psi(t_k - t_{k-1})) g_2(t_{k-1}) \sigma(t_{k-1}) + \\
&- \frac{I}{2} g_l \sum_{j=1}^{k-2} \{\Delta D(\Psi(t_k - t_{j+1})) - \Delta D(\Psi(t_k - t_j))\} \{g_2(t_{j+1})\sigma(t_{j+1}) + g_2(t_j)\sigma(t_j)\},
\end{aligned} \tag{2.17}$$

inversion of Eq.(2.16) gives a constitutive equation,

$$\sigma(t_k) = \frac{I}{\Phi(t_k)} \{ \varepsilon(t_k) - H(t_k) \}, \quad (2.18)$$

where

$$\Phi(t_k) = g_o(t_k) D_o + \frac{I}{2} g_1(t_k) g_2(t_k) \Delta D(\psi(t_k - t_{k-1})). \quad (2.19)$$

2.3. Multiaxial stresses formulation

This section presents the full details to develop a new formulation for the multiaxial constitutive relations for isotropic materials. It was assumed in this formulation that the strains (total) are known for each time increment. Also, it was assumed that the incremental strain rate is constant. These assumptions are consistent with most nonlinear constitutive models executed by using the displacement-based finite element. The constitutive equation in matrix structure can be written as follows [9],

$$\{ \sigma(t_k) \} = [M(t_k)] \{ \varepsilon(t_k) \} - \frac{I}{\Phi(t_k)} \{ H(t_k) \}, \quad (2.20)$$

where,

$$[M(t_k)] = \frac{I}{\Phi(t_k)(1-\nu^2)} \begin{bmatrix} I & \nu & 0 \\ \nu & I & 0 \\ 0 & 0 & \frac{I-\nu}{2} \end{bmatrix}, \text{ (for plane stress condition),} \quad (2.21)$$

$$[M(t_k)] = \frac{I}{\Phi(t_k)(1+\nu)(1-2\nu)} \begin{bmatrix} (1-\nu) & \nu & 0 \\ \nu & (1-\nu) & 0 \\ 0 & 0 & \frac{1-2\nu}{2} \end{bmatrix}, \text{ (for plane strain condition),} \quad (2.22)$$

2.4. Nonlinear finite element implementation

It can be written the formula of the finite element equilibrium based on the principle of virtual work as follows [12]

$$\int_V [B^T] \{ \sigma(t_k) \} dV = \{ F(t_k) \}, \quad (2.23)$$

where $\{ F(t_k) \}$ represents the vector of external force.

Equation (2.20) could not be satisfied with the nonlinear viscoelastic problem conditions. In order to overcome this issue, the incremental procedure is carried out, where the external force represents a number of small load increments. The initial increment of load starts at $(t=0)$ where the solution is known (in most cases, stress-free or simple elastic response). The form of the equilibrium for each increment is [12],

$$\int_V [B^T] \{\Delta\sigma(t_k)\} dV = \{\Delta F(t_k)\} \quad (2.24)$$

by substitution Eq.(2.20) in Eq.(2.23), then it can get the following,

$$[K(t_k)] \{\Delta u(t_k)\} = \{\Delta P(t_k)\}, \quad (2.25)$$

where

$$[K(t_k)] = \int_V [B^T] [M(t_k)] [B] dV, \quad (2.26)$$

$$\{\Delta P(t_k)\} = \{\Delta F(t_k)\} - \int_V [B^T] \{H(t_k)\} dV. \quad (2.27)$$

It should be used as an iterative procedure to ensure obtaining the equilibrium in every time increment, and this is because the equations in Eq.(2.26) are non-linear. In order to find the solution to such a problem, the modified Newton-Raphson technique is applied. Assume that the residual force vector $R^m(t)$ at time t after a number of iteration cycles (m) is [12],

$$\{R^m(t_k)\} = [K^0(t_k)] \{\Delta u^m(t_k)\} - \{\Delta P(t_k)\}. \quad (2.28)$$

When the stiffness matrix is computed, then the value of the superscript is equal to (zero). This occurs at the initial increment. It can be written the equation of the residual forces at iteration cycle ($m+1$) as [12],

$$\{R^{m+1}(t_k)\} = \{R^m(t_k)\} + \frac{dR^m(t_k)}{du^m(t_k)} \{du^m(t_k)\}. \quad (2.29)$$

Rearrange Eq.(2.29) based on Eq.(2.28), then it gives the following,

$$\{R^{m+1}(t_k)\} = \{R^m(t_k)\} + [K^0(t_k)] \{du^m(t_k)\}. \quad (2.30)$$

In order to obtain the equilibrium, it should be the residual forces reach a tolerably low level. Assume that the $R^{m+1}(t)$ is reaches zero, then Eq.(2.30) reduces to the following

$$\{du^m(t_k)\} = -[K^0(t_k)]^{-1} \{R^m(t_k)\}. \quad (2.31)$$

It can be assumed the form of the displacement increment at the subsequent iteration cycle ($m+1$) is

$$\{\Delta u^{m+1}(t_k)\} = \{\Delta u^m(t_k)\} + \{du^m(t_k)\}. \quad (2.32)$$

It can be summarized the main steps to obtain the numerical solution of the problem as follows,

- (i) Find the stiffness matrix $K^0(t)$ at the initial time increment.
- (ii) Use the iteration process by using Eqs.(2.30) to (2.31), until the following condition is met,

$$\frac{\{du^{m+1}(t_k)\}}{\{\Delta u^{m+1}(t_k)\}} < TOL, \tag{2.33}$$

where TOL is a small value (less than 0.00001). The flowchart for the numerical solution of the of nonlinear FEM for nonlinear viscoelastic material is shown in Fig.1.

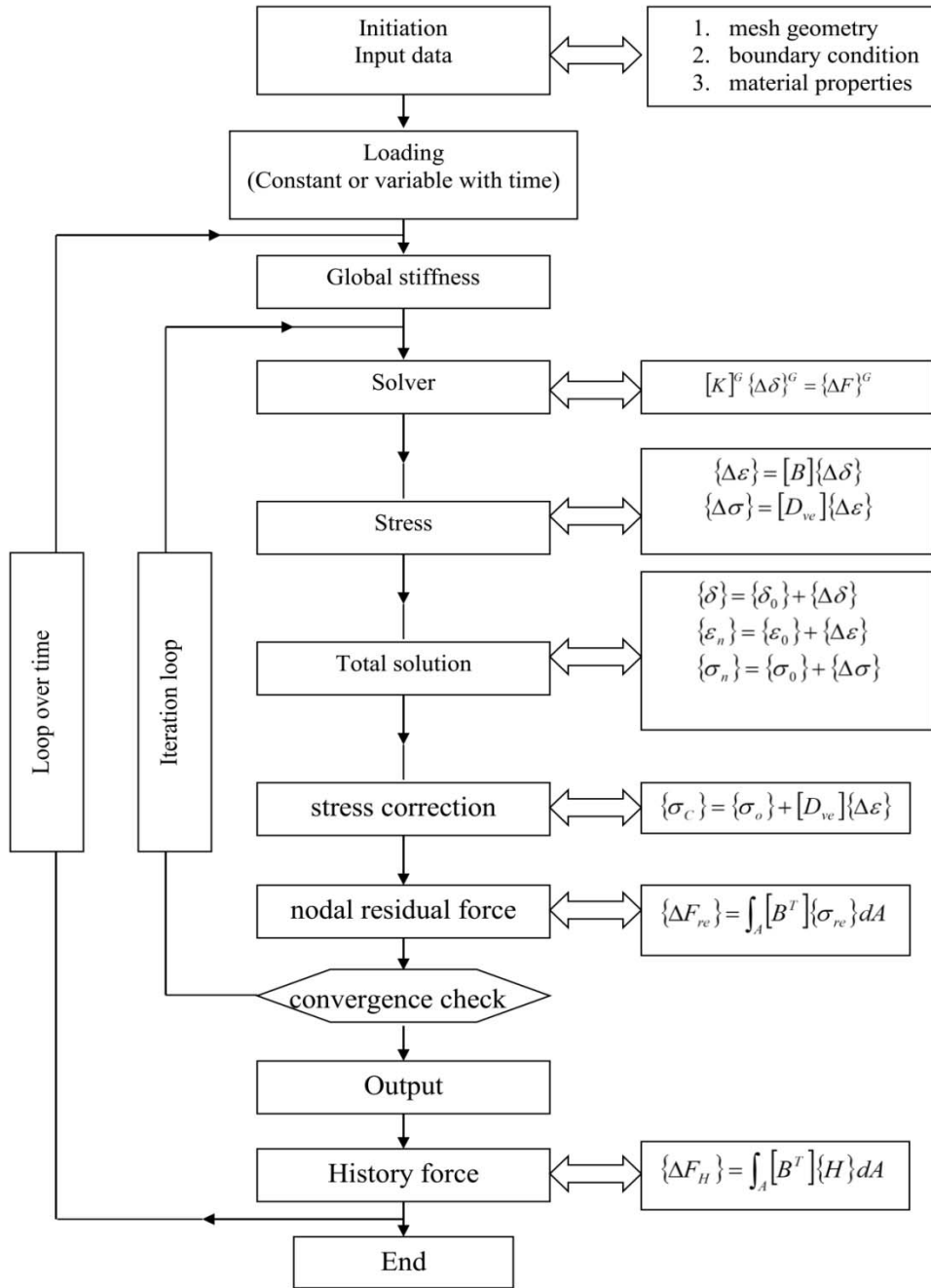


Fig.1. Flowchart of nonlinear FEM for nonlinear viscoelastic material.

3. Finite element results

The glassy amorphous polymer material (PMMA)[5] was selected as a case study to achieve the verification issue. Table 1 lists the results of the tests (calibrated elastic compliance and Prony parameters), while Tab.2 shows the nonlinear stress-dependent parameters in Schapery's equation for PMMA Polymers.

Table 1. Elastic compliance and prony series coefficient for PMMA polymer [3].

n	$\lambda_n (s^{-1})$	$D_n \times 10^{-6} (MPa^{-1})$
1	1	23.6358
2	10^{-1}	5.6602
3	10^{-2}	14.8405
4	10^{-3}	18.8848
5	10^{-4}	28.5848
6	10^{-5}	40.0569
7	10^{-6}	60.4235
8	10^{-7}	79.6477
9	10^{-8}	162.179
D_0	270.9×10^{-6}	

Table 2. The nonlinear stress-dependent parameters [3].

g_1	α_1	α_2	α_3	α_4
	0.183	0.567	-1.067	0.533
g_1	β_1	β_2	β_3	β_4
	0.067	0.133	2.133	-2.133
g_2	γ_1	γ_2	γ_3	γ_4
	-0.773	9.707	-15.787	8.533
a_σ	δ_1	δ_2	δ_3	δ_4
	-0.373	2.58	-5.227	3.52

Figure 2 shows the relationship between the nonlinear stress and Schapery's parameters based on the experimental test. It was found that the nonlinear stress-dependent parameters have acceptable values when using polynomials of 4th order in Eq.(2.3). It was determined the value of the effective stress (σ_o), it is found to be 20 MPa. (σ_o) represents the limit of the linear response. The range of effective stress was between 0 and 40 MPa, these results were obtained after calibrating the polynomial coefficients. It should be noticed that the polynomial functions are valid within the mentioned stress range; otherwise, it can't obtain the actual behavior of the material. Figure 2 shows the polynomial coefficients (calibrated) for the nonlinear parameters (4 parameters). According to the numerical test done and the experimental work by Lai and Bakker [6], it was proved that the proposed algorithm for the numerical modeling is valid.

It was selected for 30 minutes to achieve a test of a series of tensile creep, and the next step was the recovery test within 30 minutes under a number of stress levels (15-35 MPa). All these processes were done

at room temperature. It was found that the linear response occurred when the stress was lower than (20 MPa). Figures 3 and 4 illustrate the variation of the strains under the creep and recovery conditions.

Figure 5 presents other numerical predictions for the uniaxial response when two-step creep loading conditions are applied for (PMMA) polymer. It was found that the obtained prediction based on the proposed numerical approach is in excellent agreement with the experimental data.

Tensile creep and recovery tests under various stress levels at room temperature reveal a linear response below 20 MPa (Figs 3 and 4). The numerical predictions for uniaxial response during two-step creep loading conditions align excellently with experimental data (Fig.5), further validating the model.

The rectangular plate with a central hole is the other example to illustrate the results based on Schapery's approach. Figure 6 exhibits the geometry and the boundary conditions. One-quarter of the plate can be selected to simulate the problem due to the symmetry. It was applied a uniform traction force (remote) equal to (10 MPa) on the notched plate during a certain period of time. The analysis of a rectangular plate with a central hole provides insights into stress distribution, showing reductions in stress concentration on the hole's edge (Fig.6). Time-dependent stress distribution along the mid-section of the plate (Fig.7) reflects modifications during nonlinear conditions.

Figure 7 shows the reduction that occurred in the stress consternation values on the hole's edge. It can be seen the distributions of stress along the mid-section of the plate during the period of time that started at ($t = 0$) until ($t = 5000s$) in Fig.8. It can be noticed that the stress distribution modified with time in the case when the nonlinearity occurred. While the distribution of stress remained the same at any time when the viscoelastic range was within linear and relatively low nonlinear.

In elastic material, the stress depends directly on the external load; with a constant load, the stresses will be constant too. Meanwhile, in the viscoelastic material, even with constant loading, the stress is reduced in the process of so-called stress relaxation, as shown in the results of Figs 7 and 8.

Figures 9 and 10 visually represent strains at selected intervals, affirming the model's ability to capture viscoelastic behavior. The small percentage error (1%) compared to experimental data supports the accuracy of the proposed numerical approach. In summary, the comprehensive validation across various scenarios demonstrates the robustness of the numerical model in predicting nonlinear viscoelastic behavior in PMMA and complex geometries, suggesting its broad applicability in material studies and engineering simulations.

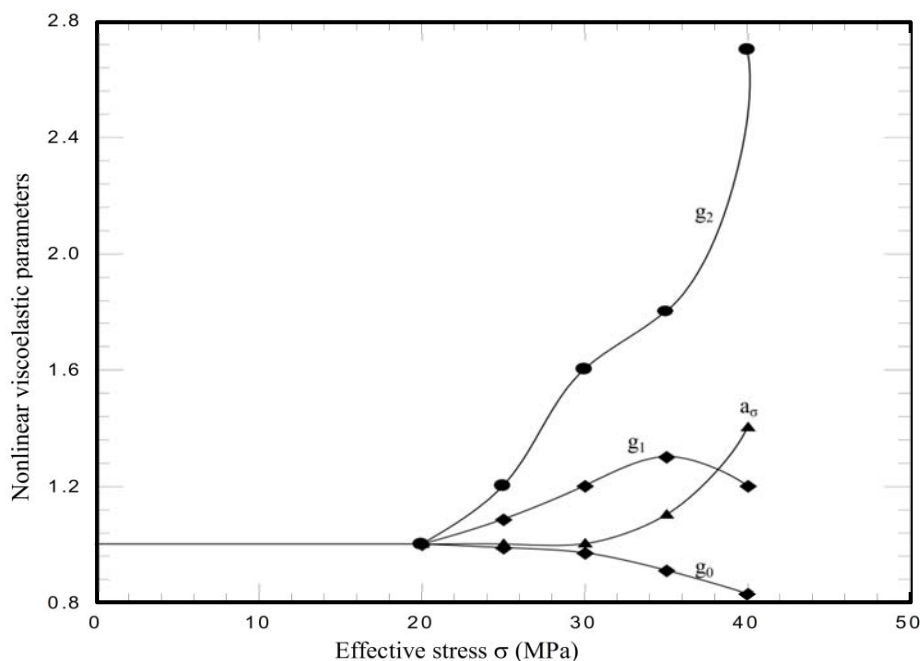


Fig.2. Nonlinear stress-dependent parameters in Schapery's equation for PMMA polymers.

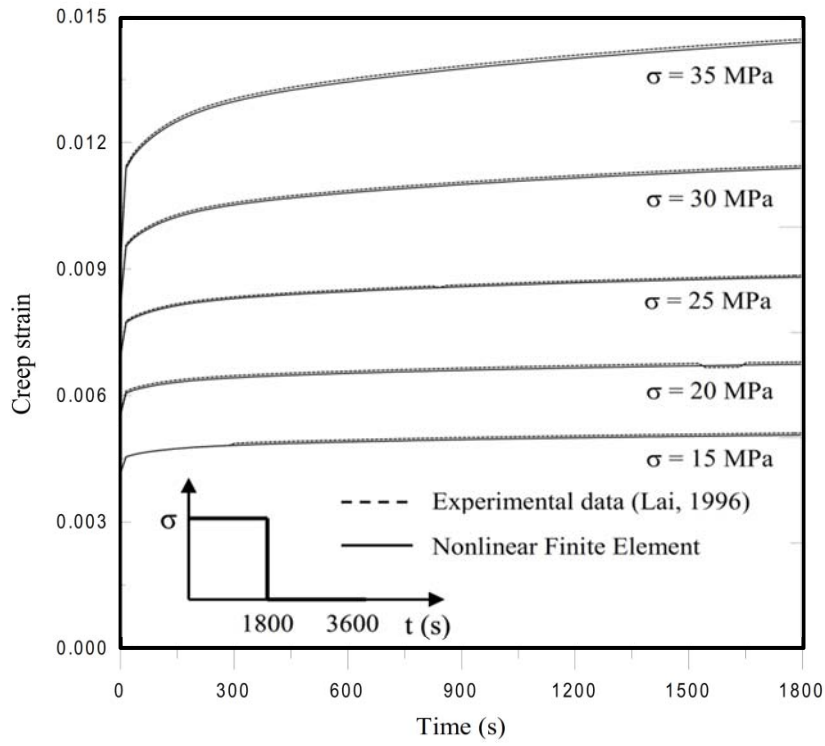


Fig.3. The creep strain for PMMA.

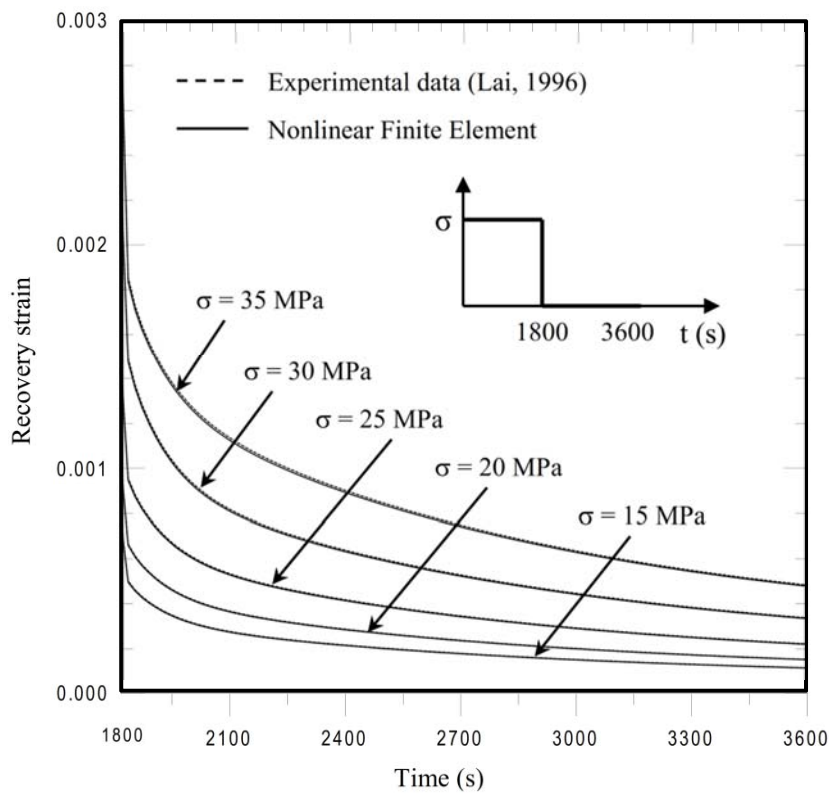


Fig.4. The recovery strain for PMMA.

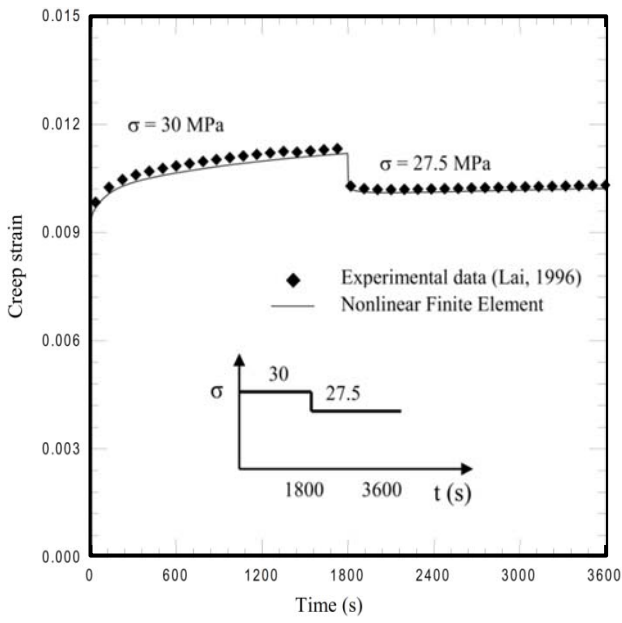


Fig.5. Two step creep response for PMMA.

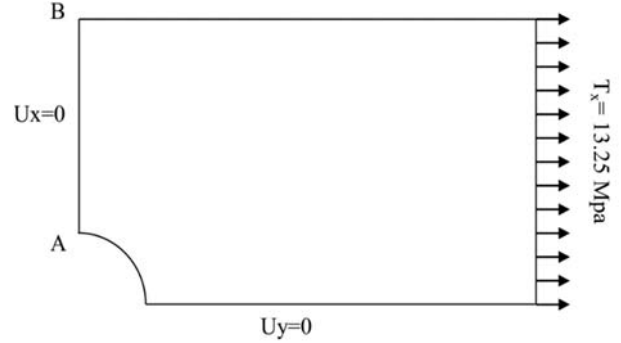


Fig.6. The configuration of rectangular plate with hole.

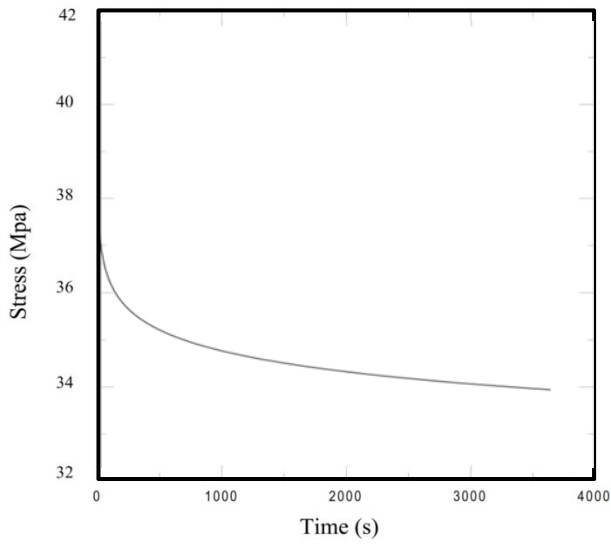


Fig.7. The reduction of stress with time in hole tip (A).

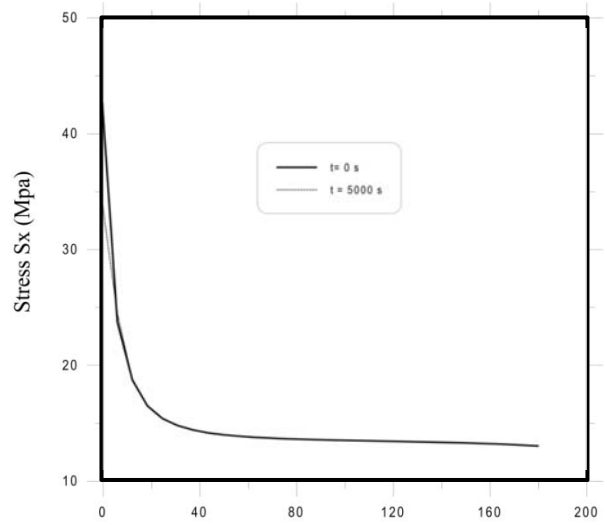


Fig.8 The distribution of stresses along path A-B.

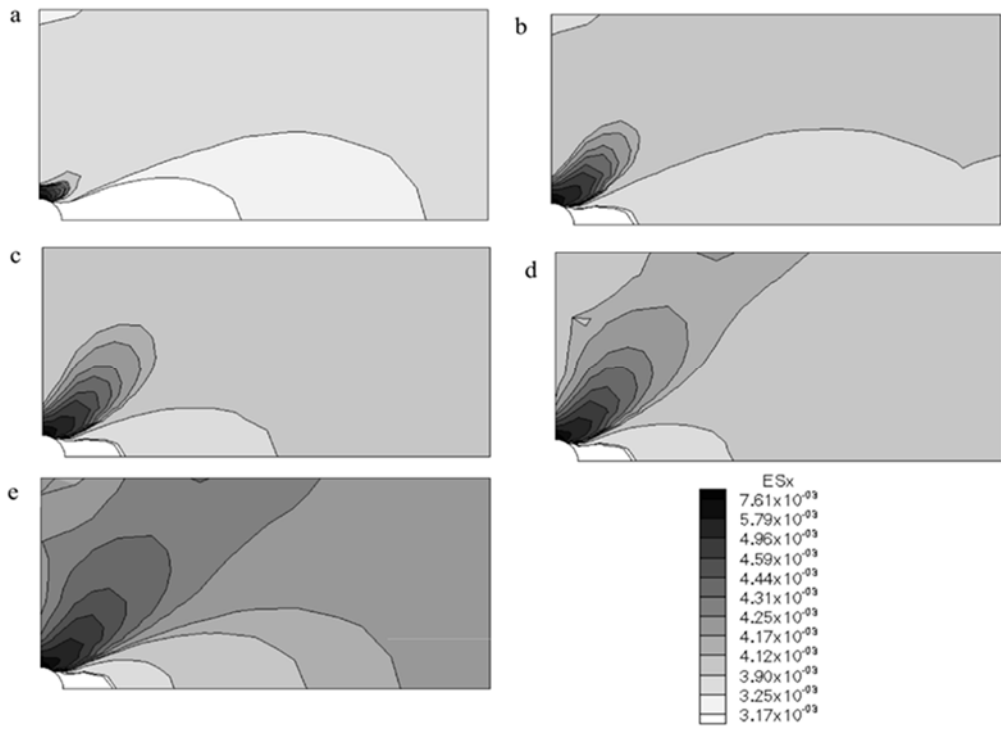


Fig.9. The strain ϵ_{xx} distribution at different times. a: 0 s; b: 500 s; c: 1000 s; d: 1800 s; e: 5000 s.

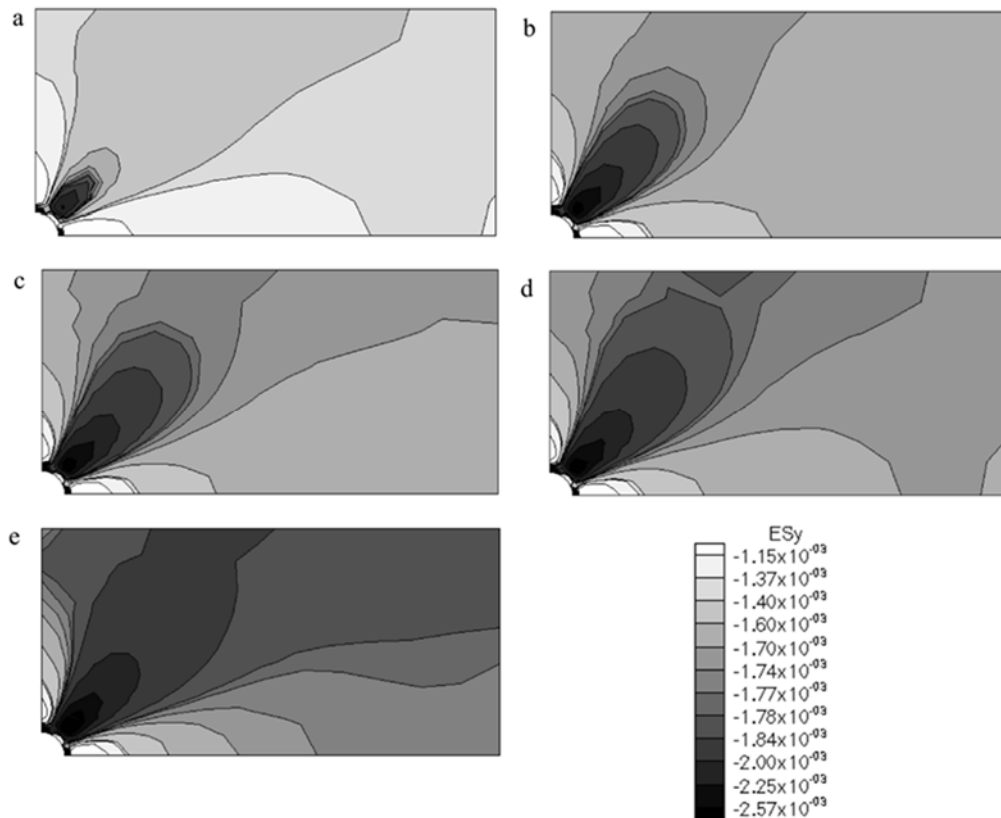


Fig.10. The strain ϵ_{yy} distribution at different times. a: 0 s; b: 500 s; c: 1000 s; d: 1800 s; e: 5000 s.

4. Conclusions and remarks

The most important conclusions obtained based on the numerical analysis can be summarized in the following points:

- Introduced a new finite element code for nonlinear viscoelastic materials based on Schapery's model. The displacement-based finite element method was applied with a modified Newton-Raphson analysis approach to overcome the material nonlinearity.
- a recursive-incremental formula was developed, which eliminates the necessity of storing full strain histories except for prior time increments, to evaluate Schapery's parameters using creep and recovery tests.
- The solution was validated, and the accuracy of the new code was about 99% based on comparisons that were made with the results of other researchers (theoretical and experimental) who used different algorithms.
- The new numerical model can be regarded as a promising tool for solving various engineering problems, including but not limited to structural mechanics, biomechanics, and civil engineering.
- The new code results provide an in-depth knowledge of viscoelastic solids and their complex behaviors, leading to enhanced design and analysis capabilities in these fields.
- The limitation of the present work is related to the material's physical properties since it was assumed an isotropic behavior. Meanwhile, some of the structures may contain composite material. The other limitation is that the current new model is valid for small deformations, but some structures may need to consider the large deformation problem to capture their response using the finite element analysis. In future work, it will be developed the new model and take these points into consideration to overcome these limitations.

Nomenclature

D_0	– instantaneous uniaxial elastic compliance ($1/MPa$)
D_n	– coefficient of the prony series ($1/MPa$)
$D(t)$	– creep compliance ($1/MPa$)
ΔD	– uniaxial transient compliance ($1/MPa$)
g_0, g_1, g_2, a_σ	– nonlinear material properties
$H(t)$	– time-dependent creep function ($1/MPa$)
t_k	– current time
$\alpha_i, \beta_i, \gamma_i, \delta_i$	– coefficients of nonlinear material properties
λ_n	– retardation time (s)
$\bar{\sigma}$	– effective octahedral shear stress
$\Phi(t)$	– time-dependent creep function ($1/MPa$)
$\psi(t)$	– reduced-time (s)

Acknowledgment

The authors acknowledge the Mechanical Engineering Department, College of Engineering, Gulf University for supporting the research work and providing facilities.

References

- [1] Bažant Z.P. (1972): *Matrix differential equation and higher-order numerical methods for problems of non-linear creep, viscoelasticity and elasto-plasticity.*– International Journal for Numerical Methods in Engineering, vol.4, No.1, pp.11-15.
- [2] Yadagiri S. and Reddy C.P. (1985): *Viscoelastic analysis of nearly incompressible solids.*– Computers & Structures, vol.20, No.5, pp.817-825.
- [3] Tressou B., Vaziri R. and Nadot-Martin C. (2018): *Application of the incremental variational approach (EIV model) to the linear viscoelastic homogenization of different types of microstructures: long fiber- particle-reinforced and strand-based composites.*– European Journal of Mechanics-A/Solids, vol.68, pp.104-116.
- [4] Henriksen M. (1984): *Nonlinear viscoelastic stress analysis-a finite element approach.*– Computers & structures, vol.18, No.1, pp.133-139.
- [5] Haj-Ali R.M. and Muliana A.H. (2004): *Numerical finite element formulation of the Schapery non-linear viscoelastic material model.*– International Journal for Numerical Methods in Engineering, vol.59, No.1, pp.25-45.
- [6] Lai J. and Bakker A. (1996): *3-D Schapery representation for non-linear viscoelasticity and finite element implementation.*– Computational mechanics, vol.18, No.3, pp.182-191.
- [7] Haj-Ali R. M. and Muliana A.H. (2003): *A micromechanical constitutive framework for the nonlinear viscoelastic behavior of pultruded composite materials.*– International Journal of Solids and Structures, vol.40, No.5, pp.1037-1057.
- [8] Muliana A., Nair A., Khan K.A. and Wagner S. (2006): *Characterization of thermo-mechanical and long-term behaviors of multi-layered composite materials.*– Composites Science and Technology, vol.66, No.15, pp.2907-2924.
- [9] Muliana A.H. and Haj-Ali R. (2008): *A multi-scale framework for layered composites with thermo-rheologically complex behaviors.*– International Journal of Solids and Structures, vol.45, No.10, pp.2937-2963.
- [10] Jabbar N.A., Hussain I.Y. Abdullah O.I. and Mohammed M.N. (2023). *An experimental investigation and numerical analysis of the thermal behavior of a clutch system using the frictional facing of functionally graded materials.*– Designs, vol.7, No.6, pp.125.
- [11] Zobeiry N., Malek S., Vaziri R. and Poursartip A. (2016): *A differential approach to finite element modelling of isotropic and transversely isotropic viscoelastic materials.*– Mechanics of Materials, vol.97, pp.76-91.
- [12] Schapery R. A. (1969): *On the characterization of nonlinear viscoelastic materials.*– Polymer Engineering & Science, vol.9, No.4, pp.295-310.
- [13] Haj-Ali, R.M. Muliana A.H. (2004). *A multi-scale constitutive formulation for the nonlinear viscoelastic analysis of laminated composite materials and structures.*– International Journal of Solids and Structures, vol.41, No.13, pp.3461-3490.
- [14] Muliana A.H. and Haj-Ali R.M. (2006): *Analysis for creep behavior and collapse of thick-section composite structures.*– Composite Structures, vol.73, No.3, pp.331-341.
- [15] Huang C.W., Abu Al-Rub R.K., Masad E.A. and Little D.N. (2011): *Three-dimensional simulations of asphalt pavement permanent deformation using a nonlinear viscoelastic and viscoplastic model.*– Journal of materials in civil engineering, vol.23, No.1, pp.56-68.
- [16] Rahmani E., Darabi M.K., Al-Rub R.K.A., Kassem E., Masad E.A. and Little D.N. (2013): *Effect of confinement pressure on the nonlinear-viscoelastic response of asphalt concrete at high temperatures.*– Construction and Building Materials, vol.47, pp.779-788.
- [17] Peña J.A., Martínez M.A. and Peña E. (2011): *A formulation to model the nonlinear viscoelastic properties of the vascular tissue.*– Acta Mechanica, vol.217, pp.63-74.
- [18] Feng H., Zhou J., Gao S. and Jiang L. (2021): *Finite element simulation of the viscoelastic behavior of elastomers under finite deformation with consideration of nonlinear material viscosity.*– Acta Mechanica, vol.232, pp.4111-4132.
- [19] Takaoka H. and Sakaue K. (2020): *Evaluation of viscoelastic-viscoplastic characteristics and finite element analyses for thermoplastics.*– Advanced Composite Materials, vol.29, No.3, pp.273-284.
- [20] Assie A.E., Eltahir M.A. and Mahmoud F.F. (2010): *The response of viscoelastic-frictionless bodies under normal impact.*– International Journal of Mechanical Sciences, vol.52, No.3, pp.446-454.
- [21] Assie A.E., Eltahir M.A. and Mahmoud F.F. (2011): *Behavior of a viscoelastic composite plates under transient load.*– Journal of Mechanical Science and Technology, vol.25, pp.1129-1140.
- [22] Ali I.A., Alazwari M.A., Eltahir M.A. and Abdelrahman A.A. (2022): *Effects of viscoelastic bonding layer on performance of piezoelectric actuator attached to elastic structure.*– Materials Research Express, vol.9, No.4, pp.045701.

- [23] Abdelrahman A.A., Nabawy A.E. Abdelhaleem A.M., Alieldin S.S. Eltaher M.A. (2020): *Nonlinear dynamics of viscoelastic flexible structural systems by finite element method.*– Engineering with Computers, vol.38, pp.169-190.
- [24] Akbaş Ş.D., Fageehi Y.A., Assie A.E. and Eltaher M.A. (2022): *Dynamic analysis of viscoelastic functionally graded porous thick beams under pulse load.*– Engineering with Computers, vol.38, pp.365-377.
- [25] Ghandourah E.E., Daikh A.A., Khatir S., Alhawsawi A.M., Banoqitah E.M. and Eltaher M.A. (2023): *A dynamic analysis of porous coated functionally graded nanoshells rested on viscoelastic medium.*– Mathematics, vol.11, No.10, pp.2407.

Received: January 6, 2024

Revised: February 15, 2024